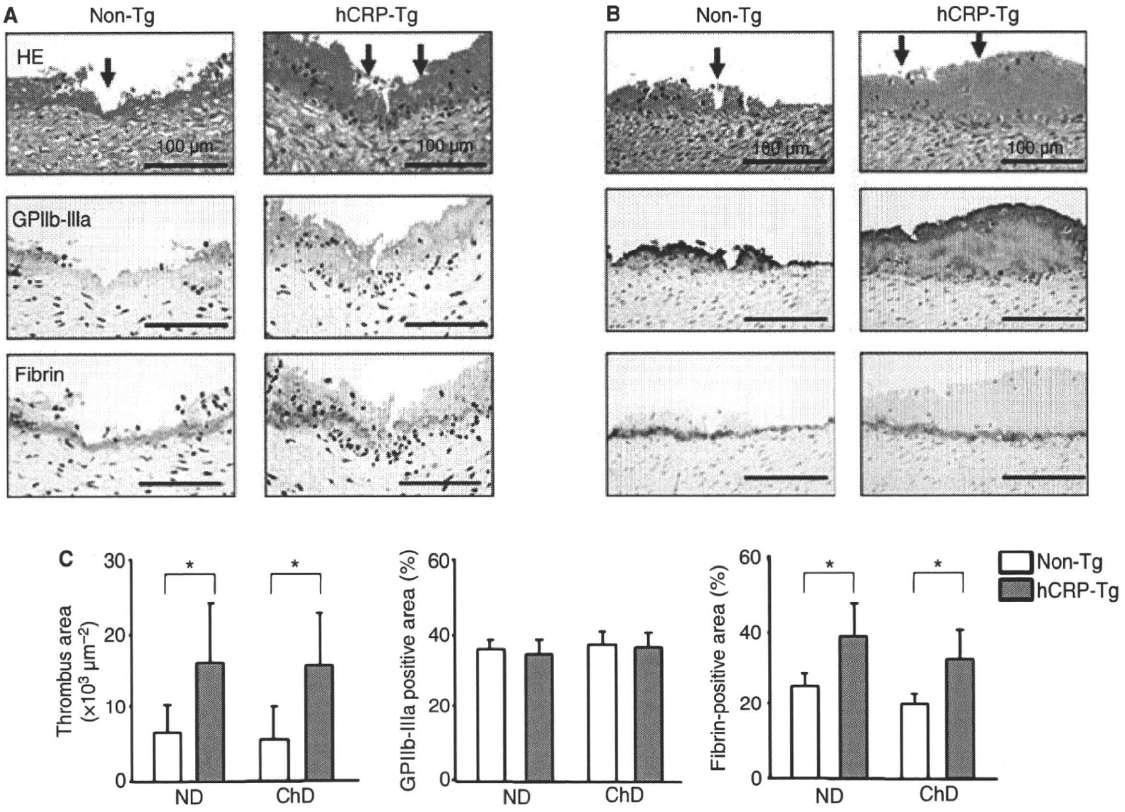

Fig. 5. Thrombus formation on neointima induced by balloon injury in femoral arteries. Thrombus size (arrows) and immunoreactive proteins of glycoprotein (GP)IIb–IIIa and fibrin on neointimas were quantified by image analysis, as described in Materials and methods (A) Thrombus formation on smooth muscle cell-rich neointima, $n = 6$ each. (B) Thrombus formation on macrophage-rich neointima, $n = 5$ each. (C) Thrombus area, GPIIB–IIIa-immunopositive-area and fibrin-immunopositive area. $^*P < 0.01$ vs. non-transgenic (Tg) rabbits. ChD, cholesterol diet; hCRP, human C-reactive protein; HE, hematoxylin and eosin; ND, normal diet.

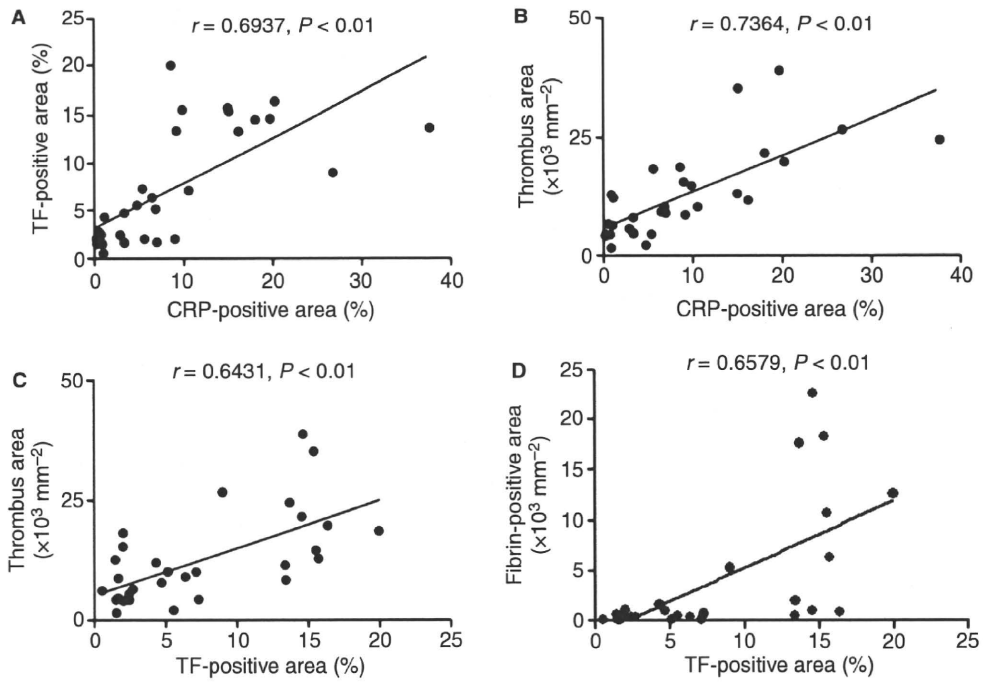

Fig. 6. Linear regression analyses of associations between C-reactive protein (CRP)-positive areas and areas of tissue factor (TF) positivity and thrombus, and between TF-positive areas and areas of fibrin positivity and thrombus ($n = 6$ each).

compared with that of non-Tg rabbits. Several mechanisms might be involved in the increased thrombogenesis in hCRP-Tg rabbits. First, elevated TF expression in neointimal SMCs induced by high levels of CRP in the lesions might directly promote thrombosis. Second, high plasma levels of CRP and lesional CRP might result in a prothrombogenic milieu in the arterial wall through reducing the level of t-PA, upregulating plasminogen activator inhibitor-1, and impairing endothelial functions [5,6]. Whether CRP itself is directly involved in the thrombosis remains unknown. Nevertheless, it is unlikely that CRP affects thrombosis by mediating platelet functions and the blood coagulation system, as we did not find any abnormalities in PT, APTT, or whole-blood hemostatic parameters. Therefore, our data do not support the notion that CRP modulates platelet activation and aggregation [6].

Thrombus size did not significantly differ between SMC-rich and macrophage-rich neointima in hCRP-Tg rabbits. Devaraj *et al.* [31] reported that CRP enhances oxidative stress and TF activity in rat peritoneal macrophages, and implied that CRP in atherosclerotic lesions affects thrombus formation after plaque disruption. Our results did not support this notion, and suggested a difference between vascular and peritoneal macrophages. Although macrophage-rich neointima develops under hyperlipidemic conditions, hCRP deposition did not enhance TF expression and thrombus formation in the lesions as compared with normolipidemic Tg rabbits. The present results could be partly explained by the effect of CRP on complement activation by enzymatically modified LDL (E-LDL). Bhakdi *et al.* [32] reported that CRP deposited in early atherosclerotic lesions is bound to E-LDL, and CRP bound to E-LDL can activate complement but inhibit the complement sequence at the stage of C3b/C5 [33]. E-LDL might reduce the biological effect of CRP in atherosclerotic lesions. The absence of additional enhancement of thrombus formation on macrophage-rich neointima suggests that CRP in macrophage-rich lesions is not thrombogenic.

The present study found higher plasma hCRP levels in hCRP-Tg rabbits than the risk levels generally proposed for humans. We could not assess which levels of CRP affect TF expression in vascular cells and thrombogenesis in vivo, and whether CRP enhances the expression of procoagulant molecules other than TF in hCRP-Tg rabbits. Future studies are required to address these issues, to confirm the roles of CRP in the development of atherothrombosis.

In conclusion, high plasma hCRP levels enhance thrombus formation in SMC-rich neointima via an increase in TF expression, but macrophage infiltration with CRP deposition in the lesions does not have additional effects. This indicates that CRP in macrophage-rich lesions might not be thrombogenic.

Addendum

S. Matsuda, A. Yamashita, S. Kitajima, T. Koike, Y. E. Chen, J. Fan and Y. Asada: contributed to the concept and design; S. Matsuda, A. Yamashita, Y. Sato, C. Sugita, S. Moriguchi-Goto, K. Hatakeyama, M. Takahashi, C. Koshimoto, Y. Matsuura, T. Iwakiri and Y. Asada: contributed to analysis and/or interpretation of data, and critical writing of the manuscript.

Acknowledgements

We thank R. Sotomura for expert technical assistance, and K. Marutsuka (University of Miyazaki), M. Morimoto (Kumamoto Health Science University) and T. Watanabe (Fukuoka Wajiro Hospital) for helpful advice and discussions. This study was supported in part by Grants-in-Aid for Scientific Research in Japan (Nos. 19790293, 20390102, and 21590374) from the Ministry of Education, Science, Sports and Culture of Japan.

Disclosure of Conflict of Interests

The authors state that they have no conflict of interest.

Supporting Information

Additional Supporting Information may be found in the online version of this article:

Data S1. Methods.
Fig. S1. Assessment of cell proliferation and apoptosis.
Fig. S2. Expression of human C-reactive protein (hCRP) and rabbit CRP (rbCRP) mRNA in liver, normal femoral arteries and femoral arteries 3 weeks after balloon injury.
Fig. S3. Platelet functions and whole-blood coagulation in human C-reactive protein (hCRP)-transgenic (Tg) and non-Tg rabbits fed with a conventional diet.
Fig. S4. Localization of C-reactive protein (CRP), tissue factor (TF) expression, thrombus formation and blood parameters in human CRP (hCRP)-transgenic (Tg) and non-Tg rabbits fed with a 0.5% cholesterol diet.
Table S1. Antibodies used for immunohistochemical staining.
Table S2. Primers used for RT-PCR analysis.
Table S3. Blood parameters in human C-reactive protein (hCRP)-transgenic (Tg) and non-Tg rabbits fed with a conventional diet.
Table S4. Blood parameters in human C-reactive protein (hCRP)-transgenic (Tg) and non-Tg rabbits fed with a 0.5% cholesterol diet.

Please note: Wiley-Blackwell are not responsible for the content or functionality of any supporting materials supplied by the authors. Any queries (other than missing material) should be directed to the corresponding author for the article.

References

1 Ridker PM. C-reactive protein and the prediction of cardiovascular events among those at intermediate risk: moving an inflammatory hypothesis toward consensus. *J Am Coll Cardiol* 2007; **49**: 2129–38.
2 Sun H, Koike T, Ichikawa T, Hatakeyama K, Shiomi M, Zhang B, Kitajima S, Morimoto M, Watanabe T, Asada Y, Chen YE, Fan J. C-reactive protein in atherosclerotic lesions: its origin and pathophysiological significance. *Am J Pathol* 2005; **167**: 1139–48.

3 Torzewski J, Torzewski M, Bowyer DE, Frohlich M, Koenig W, Waltenberger J, Fitzsimmons C, Hombach V. C-reactive protein frequently colocalizes with the terminal complement complex in the intima of early atherosclerotic lesions of human coronary arteries. *Arterioscler Thromb Vasc Biol* 1998; **18**: 1386–92.

4 Ishikawa T, Hatakeyama K, Imamura T, Date H, Shibata Y, Hikichi Y, Asada Y, Eto T. Involvement of C-reactive protein obtained by directional coronary atherectomy in plaque instability and developing restenosis in patients with stable or unstable angina pectoris. *Am J Cardiol* 2003; **91**: 287–92.

5 Verma S, Devaraj S, Jialal I. Is C-reactive protein an innocent bystander or proatherogenic culprit? C-reactive protein promotes atherothrombosis. *Circulation* 2006; **113**: 2135–50.

6 Scirica BM, Morrow DA. Is C-reactive protein an innocent bystander or proatherogenic culprit? The verdict is still out. *Circulation* 2006; **113**: 2128–34.

7 Koike T, Kitajima S, Yu Y, Nishijima K, Zhang J, Ozaki Y, Morimoto M, Watanabe T, Bhakdi S, Asada Y, Chen YE, Fan J. Human C-reactive protein does not promote atherosclerosis in transgenic rabbits. *Circulation* 2009; **120**: 2088–94.

8 Torzewski M, Reifenberg K, Cheng F, Wiese E, Küpper I, Crain J, Lackner KJ, Bhakdi S. No effect of C-reactive protein on early atherosclerosis in LDLR−/−/human C-reactive protein transgenic mice. *Thromb Haemost* 2008; **99**: 196–201.

9 Hirschfield GM, Gallimore JR, Kahan MC, Hutchinson WL, Sabin CA, Benson GM, Dhillon AP, Tennent GA, Pepys MB. Transgenic human C-reactive protein is not proatherogenic in apolipoprotein E-deficient mice. *Proc Natl Acad Sci USA* 2005; **102**: 8309–14.

10 Reifenberg K, Lehr HA, Baskal D, Wiese E, Schaefer SC, Black S, Samols D, Torzewski M, Lackner KJ, Husmann M, Blettner M, Bhakdi S. Role of C-reactive protein in atherogenesis: can the apolipoprotein E knockout mouse provide the answer? *Arterioscler Thromb Vasc Biol* 2005; **25**: 1641–6.

11 Trion A, de Maat MP, Jukema JW, van der Laarse A, Maas MC, Offerman EH, Havekes LM, Szalai AJ, Princen HM, Emeis JJ. No effect of C-reactive protein on early atherosclerosis development in apolipoprotein E*3-leiden/human C-reactive protein transgenic mice. *Arterioscler Thromb Vasc Biol* 2005; **25**: 1635–40.

12 Elliott P, Chambers JC, Zhang W, Clarke R, Hopewell JC, Peden JF, Erdmann J, Braund P, Engert JC, Bennett D, Coin L, Ashby D, Tzoulaki I, Brown IJ, Mt-Isa S, McCarthy MI, Peltonen L, Freimer NB, Farrall M, Ruokonen A, *et al.* Genetic loci associated with C-reactive protein levels and risk of coronary heart disease. *JAMA* 2009; **302**: 37–48.

13 Zacho J, Tybjaerg-Hansen A, Jensen JS, Grande P, Sillesen H, Nordestgaard BG. Genetically elevated C-reactive protein and ischemic vascular disease. *N Engl J Med* 2008; **359**: 1897–908.

14 Teoh H, Quan A, Lovren F, Wang G, Tirgari S, Szmitko PE, Szalai AJ, Ward ME, Verma S. Impaired endothelial function in C-reactive protein overexpressing mice. *Atherosclerosis* 2008; **201**: 318–25.

15 Singh U, Devaraj S, Jialal I. C-reactive protein decreases tissue plasminogen activator activity in human aortic endothelial cells: evidence that C-reactive protein is a procoagulant. *Arterioscler Thromb Vasc Biol* 2005; **25**: 2216–21.

16 Wu J, Stevenson MJ, Brown JM, Grunz EA, Strawn TL, Fay WP. C-reactive protein enhances tissue factor expression by vascular smooth muscle cells: mechanisms and in vivo significance. *Arterioscler Thromb Vasc Biol* 2008; **28**: 698–704.

17 Bisoendial RJ, Kastelein JJ, Levels JH, Zwaginga JJ, van den Bogaard B, Reitsma PH, Meijers JC, Hartman D, Levi M, Stroes ES. Activation of inflammation and coagulation after infusion of C-reactive protein in humans. *Circ Res* 2005; **96**: 714–16.

18 Danenberg HD, Szalai AJ, Swaminathan RV, Peng L, Chen Z, Seifert P, Fay WP, Simon DI, Edelman ER. Increased thrombosis after arterial injury in human C-reactive protein-transgenic mice. *Circulation* 2003; **108**: 512–15.

19 Tennent GA, Hutchinson WL, Kahan MC, Hirschfield GM, Gallimore JR, Lewin J, Sabin CA, Dhillon AP, Pepys MB. Transgenic human CRP is not pro-atherogenic, pro-atherothrombotic or pro-inflammatory in apoE−/− mice. *Atherosclerosis* 2008; **196**: 248–55.

20 Ortiz MA, Campana GL, Woods JR, Boguslawski G, Sosa MJ, Walker CL, Labarrere CA. Continuously-infused human C-reactive protein is neither proatherosclerotic nor proinflammatory in apolipoprotein E-deficient mice. *Exp Biol Med (Maywood)* 2009; **234**: 624–31.

21 Pepys MB, Baltz M, Gomer K, Davies AJ, Doenhoff M. Serum amyloid P-component is an acute-phase reactant in the mouse. *Nature* 1979; **278**: 259–61.

22 Yamashita A, Furukoji E, Marutsuka K, Hatakeyama K, Yamamoto H, Tamura S, Ikeda Y, Sumiyoshi A, Asada Y. Increased vascular wall thrombogenicity combined with reduced blood flow promotes occlusive thrombus formation in rabbit femoral artery. *Arterioscler Thromb Vasc Biol* 2004; **24**: 2420–4.

23 Yamashita A, Matsuda S, Matsumoto T, Moriguchi-Goto S, Takahashi M, Sugita C, Sumi T, Imamura T, Shima M, Kitamura K, Asada Y. Thrombin generation by intimal tissue factor contributes to thrombus formation on macrophage-rich neointima but not normal intima of hyperlipidemic rabbits. *Atherosclerosis* 2009; **206**: 418–26.

24 Marutsuka K, Hatakeyama K, Sato Y, Yamashita A, Sumiyoshi A, Asada Y. Protease-activated receptor 2 (PAR2) mediates vascular smooth muscle cell migration induced by tissue factor/factor VIIa complex. *Thromb Res* 2002; **107**: 271–6.

25 Ridker PM, Cook N. Clinical usefulness of very high and very low levels of C-reactive protein across the full range of Framingham Risk Scores. *Circulation* 2004; **109**: 1955–9.

26 Wang D, Oparil S, Chen YF, McCrory MA, Skibinski GA, Feng W, Szalai AJ. Estrogen treatment abrogates neointima formation in human C-reactive protein transgenic mice. *Arterioscler Thromb Vasc Biol* 2005; **25**: 2094–9.

27 Danenberg HD, Grad E, Swaminathan RV, Chen Z, Seifert P, Szalai AJ, Lotan C, Simon DI, Edelman ER. Neointimal formation is reduced after arterial injury in human crp transgenic mice. *Atherosclerosis* 2008; **201**: 85–91.

28 Marmur JD, Rossikhina M, Guha A, Fyfe B, Friedrich V, Mendlowitz M, Nemerson Y, Taubman MB. Tissue factor is rapidly induced in arterial smooth muscle after balloon injury. *J Clin Invest* 1993; **91**: 2253–9.

29 Asada Y, Hara S, Tsuneyoshi A, Hatakeyama K, Kisanuki A, Marutsuka K, Sato Y, Kamikubo Y, Sumiyoshi A. Fibrin-rich and platelet-rich thrombus formation on neointima: recombinant tissue factor pathway inhibitor prevents fibrin formation and neointimal development following repeated balloon injury of rabbit aorta. *Thromb Haemost* 1998; **80**: 506–11.

30 Cirillo P, Golino P, Calabrò P, Calì G, Ragni M, De Rosa S, Cimmino G, Pacileo M, De Palma R, Forte L, Gargiulo A, Corigliano FG, Angri V, Spagnuolo R, Nitsch L, Chiariello M. C-reactive protein induces tissue factor expression and promotes smooth muscle and endothelial cell proliferation. *Cardiovasc Res* 2005; **68**: 47–55.

31 Devaraj S, Dasu MR, Singh U, Rao LV, Jialal I. C-reactive protein stimulates superoxide anion release and tissue factor activity in vivo. *Atherosclerosis* 2009; **203**: 67–74.

32 Bhakdi S, Torzewski M, Klouche M, Hemmes M. Complement and atherogenesis: binding of CRP to degraded, nonoxidized LDL enhances complement activation. *Arterioscler Thromb Vasc Biol* 1999; **19**: 2348–54.

33 Bhakdi S, Torzewski M, Paprotka K, Schmitt S, Barsoom H, Suriyaphol P, Han SR, Lackner KJ, Husmann M. Possible protective role for C-reactive protein in atherogenesis: complement activation by modified lipoproteins halts before detrimental terminal sequence. *Circulation* 2004; **109**: 1870–6.

Tissue Factor Detection for Selectively Discriminating Unstable Plaques in an Atherosclerotic Rabbit Model

Takashi Temma[1], Yuki Ogawa[1], Yuji Kuge[1,2], Seigo Ishino[1], Nozomi Takai[1], Kantaro Nishigori[1], Masashi Shiomi[3], Masahiro Ono[1], and Hideo Saji[1]

[1]Department of Patho-Functional Bioanalysis, Graduate School of Pharmaceutical Sciences, Kyoto University, Sakyo-ku, Kyoto, Japan; [2]Central Institute of Isotope Science, Hokkaido University, Kita-ku, Sapporo, Japan; and [3]Institute for Experimental Animals, Kobe University Graduate School of Medicine, Chuo-ku, Kobe, Japan

Tissue factor (TF), a transmembrane glycoprotein that acts as an essential cofactor to factor VII/VIIa, initiates the exogenous blood coagulation cascade leading to thrombin generation and subsequent thrombus formation in vivo. TF expression is closely related to plaque vulnerability, and high TF expression is shown in macrophage-rich atheromatous lesions, making TF a potential target for detecting atheromatous lesions in vivo. Thus, we prepared ^{99m}Tc-labeled anti-TF-monoclonal antibody (TF-mAb) IgG as a molecular probe and evaluated its usefulness to achieve TF-specific imaging using myocardial infarction–prone Watanabe heritable hyperlipidemic (WHHLMI) rabbits. **Methods:** Anti-TF-mAb was created using a standard hybridoma technique and was labeled by ^{99m}Tc with 6-hydrazinonicotinic acid (HYNIC) as a chelating agent to obtain ^{99m}Tc-TF-mAb. The immunoreactivity of HYNIC-TF-mAb was estimated by flow cytometry. WHHLMI and control rabbits were injected intravenously with ^{99m}Tc-TF-mAb. Twenty-four hours after the injection, the aorta was removed and radioactivity was measured. Autoradiography and histologic studies were performed using serial aorta sections. Subclass matched antibody (IgG_1) was used as a negative control. **Results:** HYNIC-TF-mAb showed 93% immunoreactivity of the anti-TF-mAb. The radioactivity accumulation in WHHLMI aortas was 6.1-fold higher than that of control rabbits. Autoradiograms showed a heterogeneous distribution of radioactivity in the intima of WHHLMI aortas. Regional radioactivity accumulation was positively correlated with TF expression density ($R = 0.64$, $P < 0.0001$). The highest radioactivity accumulation in percentage injected dose × body weight/mm^2 × 10^2 was found in atheromatous lesions (5.2 ± 1.9) followed by fibroatheromatous (2.1 ± 0.7), collagen-rich (1.8 ± 0.7), and neointimal lesions (1.8 ± 0.6). In contrast, ^{99m}Tc-IgG_1 showed low radioactivity accumulation in WHHLMI aortas that was independent of the histologic grade of lesions. **Conclusion:** The TF-detecting ability and preferential accumulation in atheromatous lesions of ^{99m}Tc-TF-mAb were demonstrated, indicating its potential for selective imaging of macrophage-rich atheromatous lesions in vivo.

Key Words: tissue factor; radioimmunodetection; thrombus; atherosclerotic plaque

J Nucl Med 2010; 51:1979–1986
DOI: 10.2967/jnumed.110.081216

Thrombus formation triggered by plaque rupture is the most important mechanism leading to the onset of acute arterial disease and ischemic sudden death. Thus, the development of a method for detecting thrombus-forming vulnerable plaques before rupture has been clinically desired to more precisely estimate risk and provide effective treatment. Although several molecular imaging probes have been investigated (*1,2*), the target molecules of such probes were not directly related to the thrombotic process.

Tissue factor (TF), a transmembrane glycoprotein that acts as an essential cofactor to factor (F) VII/VIIa, initiates the exogenous blood coagulation cascade leading to thrombin generation and subsequent thrombus formation. TF expression was identified in atherosclerotic lesions, including in endothelial cells, smooth muscle cells, monocytes, and, especially, macrophages or foam cells (*3*). In human pathologic lesions, the TF content of de novo lipid-rich plaques was higher than that of stenotic fibrous plaques (*4*), and such lipid-rich plaque tissue was 6 times more thrombogenic than fibrous plaques. In addition, our recent study also demonstrated that TF expression was closely related to plaque vulnerability, with high TF expression specifically in macrophage-rich atheromatous lesions among heterogeneous atherosclerotic lesions (*5*). Given these data, TF is a potential target for probes detecting atheromatous lesions at higher risk for rupture in vivo.

In the present study, we prepared a monoclonal antibody to TF (TF-mAb) and labeled it with ^{99m}Tc (^{99m}Tc-TF-mAb) as a molecular probe. Using an atherosclerosis model (myocardial infarction–prone Watanabe heritable hyperlipidemic [WHHLMI] rabbits) (*6*), we investigated the accumulation of ^{99m}Tc-TF-mAb in atherosclerotic lesions in comparison with histologic characteristics and evaluated the potential of ^{99m}Tc-TF-mAb as a molecular probe for detecting vulnerable atheromatous lesions.

Received Jul. 13, 2010; revision accepted Sep. 8, 2010.
For correspondence or reprints contact: Yuji Kuge, Central Institute of Isotope Science, Hokkaido University, Kita 15 Nishi 7, Kita-ku, Sapporo 060-8638, Japan.
E-mail: kuge@ric.hokudai.ac.jp

MATERIALS AND METHODS

Design and Preparation of ^{99m}Tc-TF-mAb and ^{99m}Tc-IgG$_1$

A monoclonal antibody (mouse IgG$_1$ subclass) for rabbit TF (193Ser-207Cys, extracellular domain) was established using a standard hybridoma technique. ^{99m}Tc-pertechnetate was eluted in saline solution on a daily basis from ^{99}Mo–^{99m}Tc generators (Ultra-Techne Kow; FUJIFILM RI Pharma Co., Ltd.).

Anti-TF-mAb was radiolabeled with ^{99m}Tc (^{99m}Tc-TF-mAb) after derivatization with 6-hydrazinonicotinic acid (HYNIC) (*7*), as previously reported (*8*). In brief, HYNIC-*N*-hydroxysuccinimide was reacted with TF-mAb, and the mixture was purified by size-exclusion filtration with a diafiltration membrane (Amicon Ultra 4 [molecular weight cutoff, 30,000]; Millipore Co.). An equal volume of ^{99m}Tc-(tricine)$_2$, prepared by the method of Larsen et al. (*9*), was added to the purified solution of HYNIC-TF-mAb to obtain ^{99m}Tc-TF-mAb. After purification by size-exclusion filtration with a PD-10 column, the radiochemical purity of ^{99m}Tc-TF-mAb was more than 95% by another size-exclusion filtration.

For the control study, negative control mouse IgG$_1$ (0102-01; Southern Biotechnology Associates Inc.) was used for the preparation of ^{99m}Tc-IgG$_1$. The radiochemical purity of ^{99m}Tc-IgG$_1$ was also estimated to be more than 95%.

Animals

All animal procedures were approved by the Kyoto University Animal Care Committee. Three male Japanese White rabbits (age, 3 mo) were used to obtain peritoneal macrophages. For biodistribution studies of ^{99m}Tc-TF-mAb, 5 WHHLMI rabbits (4 male, 1 female; age, 12–18 mo; mean weight ± SD, 3.4 ± 0.2 kg; supplied by the Institute for Experimental Animals, Kobe University School of Medicine, Japan) were used. Four male Japanese White rabbits (age, 3 mo; mean weight ± SD, 1.9 ± 0.2 kg) were used for the control study. For ^{99m}Tc-IgG$_1$ studies, 3 WHHLMI rabbits (1 male and 2 female; age, 11–12 mo; mean weight ± SD, 3.2 ± 0.1 kg) were used. The animals were fed standard chow and given water ad libitum.

Immunoreactivity of HYNIC-TF-mAb

Rabbit peritoneal macrophages were obtained by the method of Ishii et al. (*10*), with minor modifications. Cells were suspended at a final concentration of 2.5×10^6 cells/mL in medium A (Dulbecco's modified Eagle's medium containing 1 mM glutamine, 100 U of penicillin per milliliter, 100 mg of streptomycin per milliliter [pH 7.4], and 0.2% lactalbumin hydrolysate). Aliquots of the cell suspension were cultured in plastic petri dishes in a humidified 5% CO_2 incubator at 37°C. After 2 h, each dish was washed twice with 10 mL of medium A to remove nonadherent cells. Monolayers were cultured for 18 h at 37°C in 20 mL of medium A, and cells were washed twice with 10 mL of medium A and then used for experiments. More than 95% of the cells were viable, as determined by a trypan blue exclusion test, and almost all of the attached cells showed positive nonspecific esterase staining.

Antibodies (5 μg/mL, 100 μL; TF-mAb, HYNIC-TF-mAb, or negative control IgG$_1$) were added to the cells (10^6) and incubated for 30 min at 4°C. After cells were washed, Alexa Fluor 488 goat antimouse IgG antibody (x0931; DakoCytomation) (10 μg/mL, 100 μL) was added for 30 min at 4°C. Fluorescence levels were measured using a flow cytometer (Becton Dickinson Inc.). Data were analyzed using BD CellQuest Pro (BD Biosciences), and an immunoreactivity index was calculated as the ratio of the median fluorescence intensity for either TF-mAb or HYNIC-TF-mAb to that of negative-control IgG$_1$. Measurements were performed 3 times per rabbit using 3 Japanese White rabbits, and the ratios were expressed as mean ± SD.

Biodistribution Studies

A simple schematic of our experimental protocol is shown in Figure 1. After 12 h of fasting, rabbits were initially anesthetized with ketamine (intramuscularly, 35 mg/kg) and xylazine (intramuscularly, 5 mg/kg). Either ^{99m}Tc-TF-mAb (547–1,024 MBq,

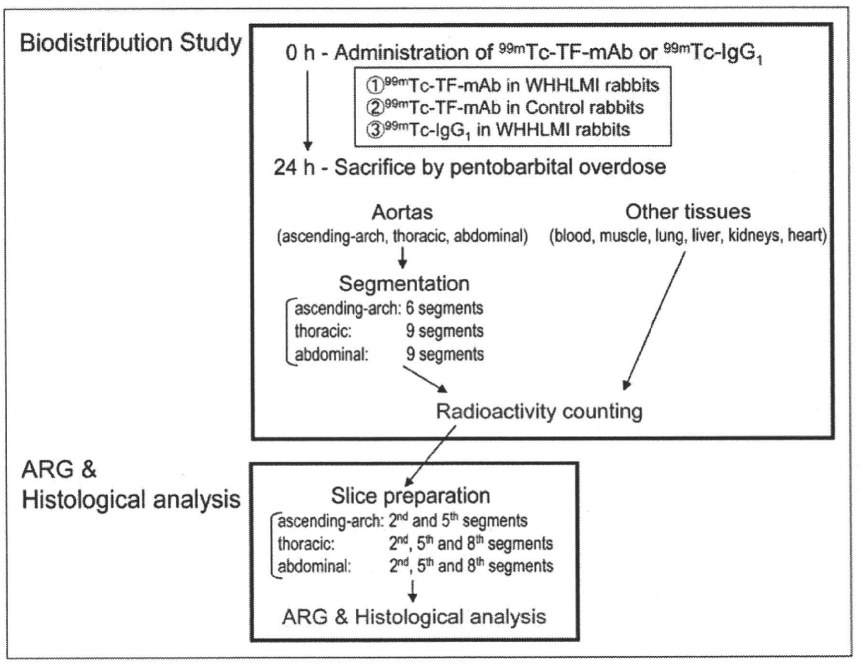

FIGURE 1. Simple schematic of this study. ARG = autoradiography.

300 μg) or ^{99m}Tc-IgG$_1$ (848–1,038 MBq, 300 μg) was injected into a marginal ear vein (5 WHHLMI rabbits and 4 control rabbits for the ^{99m}Tc-TF-mAb study, 3 WHHLMI rabbits for the ^{99m}Tc-IgG$_1$ study). Twenty-four hours after the injection, animals were sacrificed by pentobarbital overdose. The ascending-arch, thoracic, and abdominal aortas, blood, and other tissues (muscle, lung, liver, kidneys, and heart) were removed. The ascending-arch aortas were divided into 6 segments, and the thoracic and abdominal aortas were divided into 9 segments. Each segment was weighed and immediately fixed in a solution containing L-(+)-lysine hydrochloride (75 mM) and 4% paraformaldehyde in phosphate buffer (37.5 mM, pH 7.4) (*11*). The radioactivity of each sample was measured with a well-type γ-counter (1480 Wizard 3″; PerkinElmer Japan Co.). The results were expressed as the differential uptake ratio (DUR), calculated as (tissue activity/tissue weight)/(injected radiotracer activity/animal body weight), with activities given in becquerels and weights in grams. The aorta-to-blood (A/B) ratio and the aorta-to-muscle (A/M) ratio were calculated from the DUR for each tissue sample.

Autoradiography

Eight segments, the second and fifth segments of the ascending aortic arch and the second, fifth, and eighth segments from the thoracic and the abdominal aortas, from each animal were used for autoradiography studies. These segments were frozen and cut into 20-μm-thick slices with a cryomicrotome. The sections were thawed and mounted on silane-coated slides, which were then placed on a phosphor image plate (Fuji Imaging Plate BAS-MS; Fuji Photo Film) for 24 h together with a calibrated standard ($^{99m}TcO_4^-$ solution). The autoradiography images were analyzed with a computerized imaging analysis system (Bio Imaging Analyzer BAS2500 and Image Gauge Software; Fuji Photo Film). The radioactivity in each region of interest was expressed as percentage injected dose × body weight/mm^2, calculated as (radioactivity in the region of interest)/(injected radioactivity/animal body weight).

Histologic Analysis

The tissue sections used for autoradiography studies were also subjected to Azan–Mallory and hematoxylin and eosin staining. Serial sections of the slices from the autoradiography studies were subjected to immunohistochemical staining (for TF, macrophages, and smooth muscle cells) using specific antibodies and an Envision+ kit (Dako) with hematoxylin counterstaining. The antibodies used were TF-mAb (4510; American Diagnostica Inc.), rabbit macrophage–specific mAb RAM-11 (Dako), and human smooth-muscle actin–specific mAb 1A4 (Dako). Immunostaining with subclass-matched irrelevant IgG served as a negative control. Azan–Mallory and hematoxylin and eosin staining were performed by standard procedures. TF expression density was determined as a percentage of the positively stained region using a VHX digital microscope (Keyence Corp.).

Classification of Atherosclerotic Lesions

We divided atherosclerotic lesions in WHHLMI rabbits into the following 4 categories, using a classification scheme based on the recommendations of the American Heart Association (*12,13*) and Azan–Mallory and hematoxylin and eosin staining, as previously described (*14–17*): neointimal (types I–III), atheromatous (type IV), fibroatheromatous (types Va and Vb), and collagen-rich (type Vc). Supplemental Figures 1A–1P (supplemental materials are available online only at http://jnm.snmjournals.org) show representative photomicrographs of the histologic features of each atherosclerotic lesion category in WHHLMI rabbits.

Regions of interest were placed to cover each atherosclerotic lesion in the aortic section of the WHHLMI rabbit and then transferred to the corresponding autoradiography images (Supplemental Figs. 1Q–1S).

Vulnerability Index

An index of morphologic destabilization characteristics, the vulnerability index, was calculated for each lesion in the WHHLMI rabbits by the method of Shiomi et al. (*18*). The vulnerability index was defined as the ratio of the lipid component area (macrophages and extracellular lipid deposits) to the fibromuscular component area (smooth muscle cells and collagen fibers). Collagen fibers and extracellular lipid deposits (extracellular vacuoles and lacunae) were determined with Azan–Mallory stain-

TABLE 1
Accumulation Levels of ^{99m}Tc-TF-mAb and ^{99m}Tc-IgG$_1$ in Aortic Segments of Control and WHHLMI Rabbits at 24 Hours After Injection

Segments	^{99m}Tc-TF-mAb		^{99m}Tc-IgG$_1$, WHHLMI
	Control	WHHLMI	
Ascending arch	0.60 ± 0.05	3.08 ± 0.57*†	2.05 ± 0.42*
Thoracic	0.51 ± 0.11	3.07 ± 1.44*‡	1.60 ± 0.44*
Abdominal	0.35 ± 0.06	2.49 ± 0.64*‡	0.76 ± 0.16*
Total	0.47 ± 0.04	2.86 ± 0.85*‡	1.40 ± 0.24*
Blood	4.0 ± 0.6	7.5 ± 0.0*	7.1 ± 0.7§
Femoral muscle	0.6 ± 0.5	0.3 ± 0.2	0.4 ± 0.1
Aorta-to-blood ratio	0.12 ± 0.02	0.38 ± 0.09*‡	0.20 ± 0.02*
Aorta-to-muscle ratio	1.0 ± 0.6	19.3 ± 19.1*‡	4.0 ± 0.4*

*$P < 0.0001$ vs. control rabbits in ^{99m}Tc-TF-mAb study.
†$P < 0.001$ vs. WHHLMI rabbits in ^{99m}Tc-IgG$_1$ study.
‡$P < 0.0001$ vs. WHHLMI rabbits in ^{99m}Tc-IgG$_1$ study.
§$P < 0.001$, vs. control rabbits in ^{99m}Tc-TF-mAb study.
Data are represented as mean ± SD of DUR.

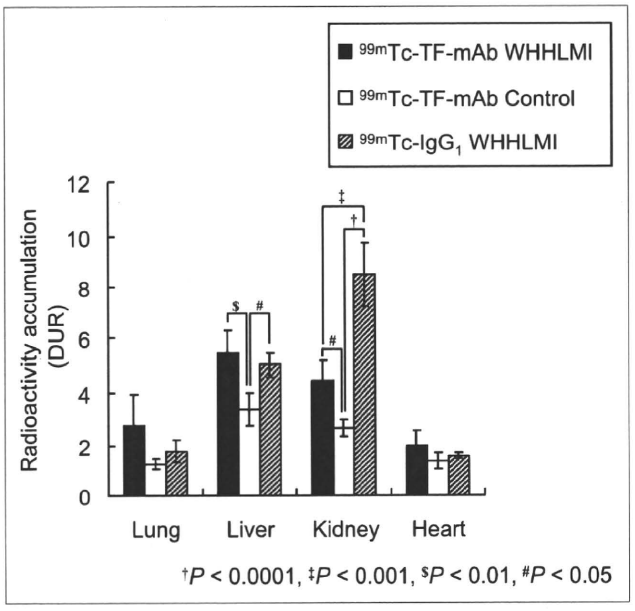

FIGURE 2. Radioactivity distribution in lung, liver, kidneys, and heart. Data are mean ± SD. †$P < 0.0001$. ‡$P < 0.001$. $$P < 0.01$. #$P < 0.05$.

ing. Macrophages and smooth muscle cells were determined with immunohistochemical staining (*17*).

Statistical Analysis

Data are presented as mean ± SD. Statistical analysis was performed with the Mann–Whitney *U* test to compare aortic segments of WHHLMI and control rabbits (Table 1). Radioactivity that accumulated in nontargeted organs among antibodies and animals was compared using 1-way ANOVA, with post hoc analysis by the Holm test (Fig. 2). Correlation coefficients were assessed by Spearman rank correlation coefficients (Fig. 3). Lesion types were compared using the Kruskal–Wallis test, with post hoc analysis by the Scheffé test (Fig. 4). A 2-tailed value of *P* less than 0.05 was considered statistically significant.

RESULTS

Immunoreactivity of HYNIC-TF-mAb

Using fluorescent-activated cell sorter analysis of rabbit peritoneal macrophages, we could clearly distinguish the signals of TF-mAb and HYNIC-TF-mAb from that of the negative control IgG_1. The median fluorescence intensity ratios of TF-mAb and HYNIC-TF-mAb to control IgG_1 were 2.90 ± 0.06 and 2.69 ± 0.11, respectively, and the difference between the labeled and unlabeled TF antibodies was not statistically significant.

Biodistribution Studies

Accumulation levels of ^{99m}Tc-TF-mAb and ^{99m}Tc-IgG_1 in the aortic segments of WHHLMI and control rabbits are summarized in Table 1. The accumulation level of ^{99m}Tc-TF-mAb in each aortic segment of WHHLMI rabbits (ascending arch, 3.08 ± 0.57 DUR; thoracic, 3.07 ± 1.44 DUR; and abdominal, 2.49 ± 0.64 DUR) was 5.1- to 7.1-fold higher than that of control rabbits (ascending arch, 0.60 ± 0.05 DUR; thoracic, 0.51 ± 0.11 DUR; and abdominal, 0.35 ± 0.06 DUR), and the differences were significant in each case. Blood-pool radioactivity levels of ^{99m}Tc-TF-mAb at 24 h were 7.5 ± 0.0 and 4.0 ± 0.6 DUR in WHHLMI and control rabbits, respectively. A/B and A/M ratios were significantly higher in WHHLMI rabbits than in control rabbits (A/B, 0.38 ± 0.09 in WHHLMI and 0.12 ± 0.02 in control rabbits; A/M, 19.3 ± 19.1 in WHHLMI and 1.0 ± 0.6 in control rabbits). In addition, the level of ^{99m}Tc-TF-mAb accumulation in WHHLMI rabbit aortas was 1.5- to 3.3-fold higher than the level of ^{99m}Tc-IgG_1 accumulation, and the differences were significant.

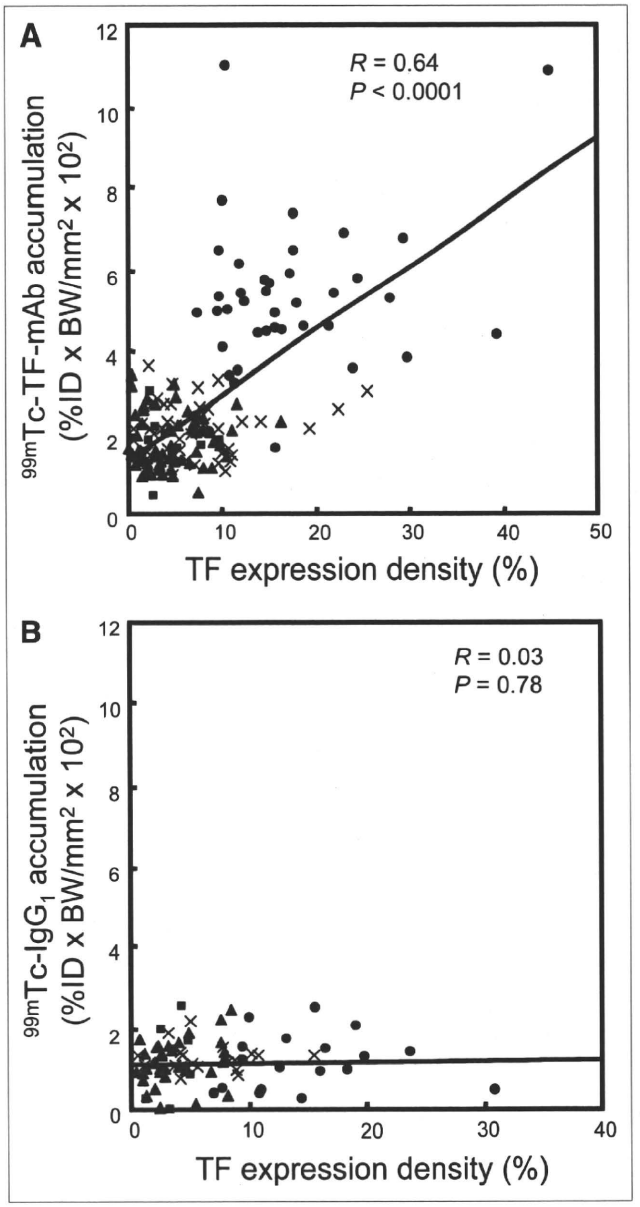

FIGURE 3. Regression analyses of TF expression density with ^{99m}Tc-TF-mAb (A) and ^{99m}Tc-IgG_1 (B) accumulation. ■ = neointimal lesion; ● = atheromatous lesion; × = fibroatheromatous lesion; ▲ = collagen-rich lesion.

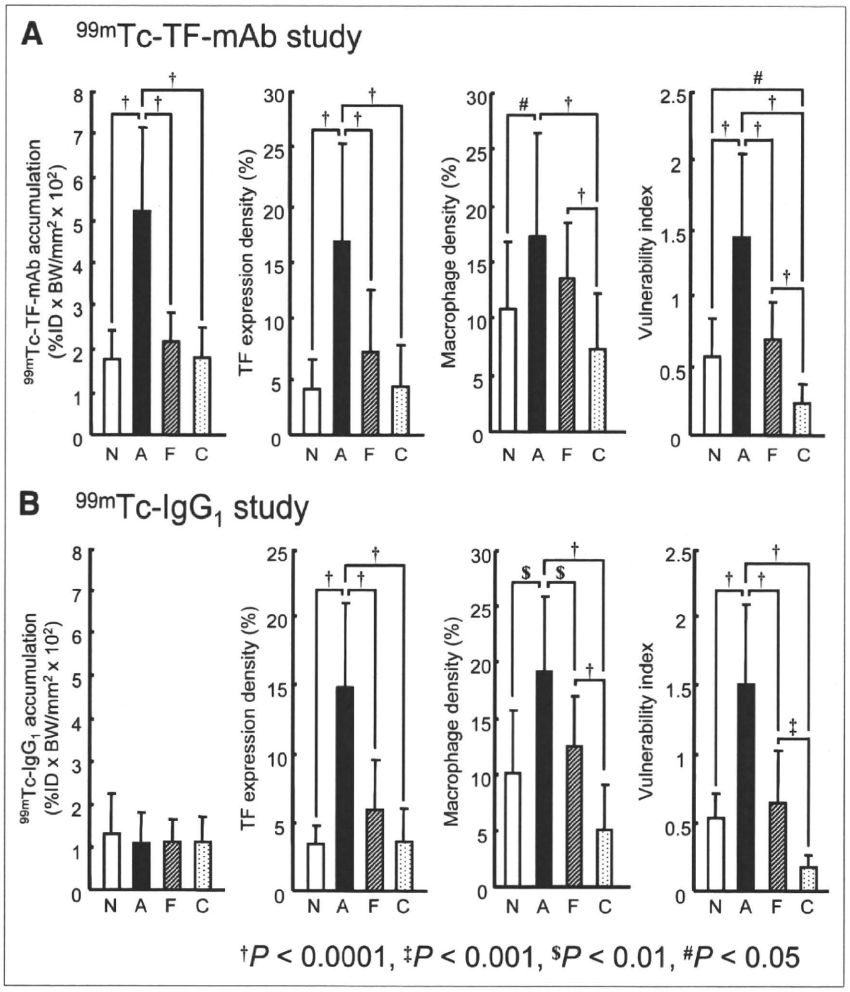

FIGURE 4. Distribution profiles of radioactivity accumulation, TF expression, macrophage density, and vulnerability index in atherosclerotic lesions in ^{99m}Tc-TF-mAb (A) and ^{99m}Tc-IgG$_1$ (B) study. A = atheromatous lesions; C = collagen-rich lesions; F = fibroatheromatous lesions; N = neointimal lesions. Data are represented as mean ± SD.

Relatively high radioactivity accumulations were found in the liver and kidneys of all 3 groups (Fig. 2). We observed that the ^{99m}Tc-TF-mAb cleared rather more slowly from the bodies of WHHLMI rabbits than from control rabbits.

Regional Distribution of ^{99m}Tc-TF-mAb, in Comparison with TF Expression

In the autoradiography study, heterogeneous ^{99m}Tc-TF-mAb accumulation was observed in the intima of WHHLMI rabbit aortas (Fig. 5B), whereas no marked accumulation was found in the aortas of control rabbits (Fig. 5A). Variable TF expression was detected in the intimal regions of the WHHLMI rabbit aorta (Figs. 5D, 5F, and 5G). Higher accumulation levels of ^{99m}Tc-TF-mAb were found in regions with high TF expression, whereas lower accumulation was observed in regions with low TF expression (Fig. 5, compare 5B with 5F and 5G). Consequently, regional ^{99m}Tc-TF-mAb accumulation levels in the aorta section were positively correlated with TF expression density in WHHLMI rabbits ($R = 0.64$, $P < 0.0001$) (Fig. 3A). No obvious TF expression was observed in the aorta of control rabbits (Figs. 5C, 5E, and 3B).

Relationship Between ^{99m}Tc-TF-mAb Accumulation and Histologic Characteristics

The plaques were categorized according to histopathologic classification criteria as follows: neointimal ($n = 12$ for ^{99m}Tc-TF-mAb study and $n = 7$ for ^{99m}Tc-IgG$_1$ study), atheromatous ($n = 40$ for ^{99m}Tc-TF-mAb study and $n = 20$ for ^{99m}Tc-IgG$_1$ study), fibroatheromatous ($n = 43$ for ^{99m}Tc-TF-mAb study and $n = 21$ for ^{99m}Tc-IgG$_1$ study), and collagen-rich ($n = 62$ for ^{99m}Tc-TF-mAb study and $n = 36$ for ^{99m}Tc-IgG$_1$ study). No lesions showed hemorrhage, plaque rupture, or thrombi (type VI). The level of ^{99m}Tc-TF-mAb accumulation was dependent on the histologic grade of the lesions (Fig. 4A) and was prominently and significantly the highest ($P < 0.0001$) in atheromatous lesions (type IV), compared with other lesions. The accumulation level of ^{99m}Tc-TF-mAb was 3.0-, 2.4-, and 2.9-fold higher in atheromatous lesions than in neointimal, fibroatheromatous, and collagen-rich lesions, respectively. The vulnerability index was also the highest in atheromatous lesions, followed in decreasing order by fibroatheromatous, neointimal, and collagen-rich lesions. Consequently, the highest level of ^{99m}Tc-TF-mAb accumulation and the highest vulnerability

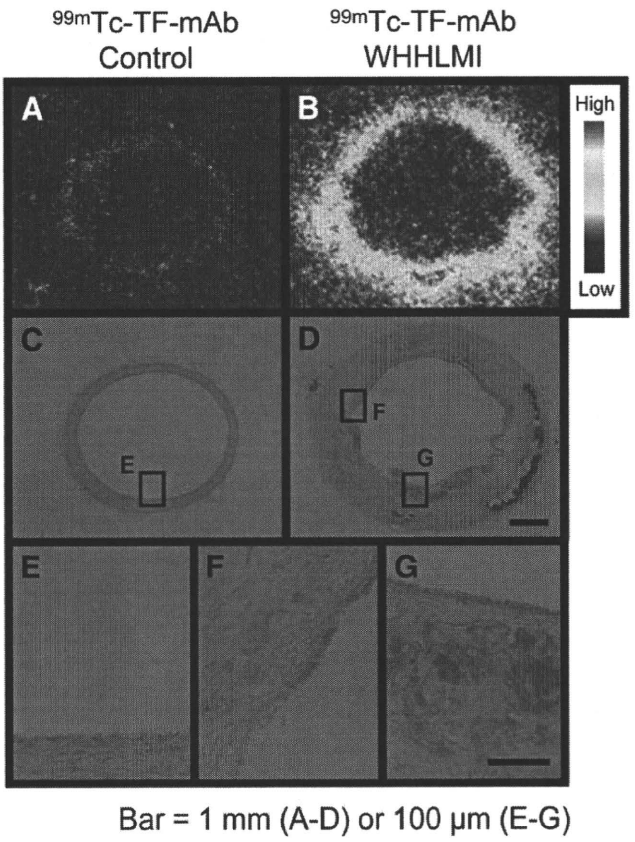

FIGURE 5. Regional distribution of ^{99m}Tc-TF-mAb and TF expression in aortic sections. Autoradiogram (A and B) and TF immunohistochemical staining (C–G) of control (C and E) and WHHLMI rabbits (D, F, and G). (E–G) High-magnification images of TF immunohistochemical staining in regions depicted in C and D. Identical color window was applied to both autoradiographic images (A and B). Bar = 1 mm (A–D) and 100 μm (E–G).

index were both observed in atheromatous lesions. In contrast, ^{99m}Tc-IgG$_1$ accumulation in lesions was low and did not correlate with the histologic grade of lesions, with no significant differences among the lesion types (Fig. 4B).

DISCUSSION

In the present study, we designed a new imaging agent, ^{99m}Tc-TF-mAb, for the purpose of discriminating atherosclerotic lesions at higher risk for rupture (thrombogenic atheromatous lesions) from more stable lesions and evaluated the potential of ^{99m}Tc-TF-mAb using an atherosclerotic rabbit model. Our major findings are that a positive correlation was demonstrated between regional ^{99m}Tc-TF-mAb accumulation and TF expression density in atherosclerotic lesions of WHHLMI rabbits but not with ^{99m}Tc-IgG$_1$ and that significantly higher ^{99m}Tc-TF-mAb accumulation was found in grade IV, more vulnerable atheromatous lesions, than in neointimal lesions or other more stable lesions. Thus, we demonstrate the potential of ^{99m}Tc-TF-mAb for molecular imaging of TF expression and selectively detecting atheromatous plaques at higher risk for rupture.

Immunoreactivity and Specificity of ^{99m}Tc-TF-mAb

Immunoreactivity, specificity, and detectable but functionally silent labeling are indispensable prerequisites of in vivo molecular imaging probes using immunodetection. In this study, flow cytometric analyses indicated that modification of TF-mAb with HYNIC did not significantly affect the immunoreactivity of the original TF-mAb. In addition, autoradiography and immunohistochemical studies showed that ^{99m}Tc-TF-mAb accumulation in atherosclerotic lesions correlated well with TF expression density, which was higher in atheromatous lesions, as expected (Figs. 3A and 4A). Further, contrary to the results with ^{99m}Tc-TF-mAb (Fig. 4A), the results with ^{99m}Tc-IgG$_1$ (Fig. 4B) showed that accumulation of ^{99m}Tc-labeled nonspecific IgG in atheromatous lesions was not significantly different from that in other types of lesions (i.e., neointimal, fibroatheromatous, and collagen-rich lesions). These findings strongly suggest the potential of ^{99m}Tc-TF-mAb to specifically recognize TF in vivo.

TF as a Target Molecule for Plaque Imaging

TF, selected as a target molecule for molecular imaging in this study, initiates the exogenous blood coagulation cascade leading to thrombus formation in vivo and represents a good marker for late-stage vulnerable lesions. TF in atherosclerotic lesions was identified in several cell types, such as endothelial cells, smooth muscle cells, monocytes, macrophages, and foam cells (*3*), similar to lectinlike oxidized low-density lipoprotein receptor 1 (LOX-1). TF expression is reported to be increased in the later stages of atheromatous progression and thus was selectively detected in atheromatous lesions in this report (Fig. 4). These findings are comparable to those of our previous immunohistochemical study (*5*) and another human study (*4*). On these bases, TF should be a potential target for detecting atheromatous plaques at higher risk for rupture in vivo. To our knowledge, this is the first report of the development of an in vivo TF imaging probe.

On the other hand, a series of imaging agents has targeted fibrin and factor XIII in thrombi using antibodies or peptides (*1*), with at least partial success. In the blood-coagulation cascade, TF initiates the system, and factor XIII covalently cross-links fibrin polymers and renders the thrombus more resistant to lysis. Therefore, ^{99m}Tc-TF-mAb will be useful for the early detection of the cascade, and fibrin and factor XIII imaging probes can detect later stages and thrombi themselves. In this study, ^{99m}Tc-TF-mAb corresponded with TF expression and showed preferential accumulation in atheromatous lesions and in lesions with increased vulnerability. Although further studies are required to investigate which target molecules in the cascade are most appropriate to estimate how unstable or vulnerable a plaque is in vivo, TF is a potential target. Furthermore, because great efforts have been made in the development of anticoagulation and antiplatelet pharmaceuticals for the treatment of atherosclerosis and

hyperlipidemia, effective imaging probes to target blood-coagulation cascades are also required for efficient drug development.

Limitations of ^{99m}Tc-TF-mAb

One drawback of ^{99m}Tc-TF-mAb is its relatively slow clearance from the blood, which is an intrinsic problem of molecular probes using antibodies. Recent advances in antibody engineering, however, should provide a promising solution for this issue. Radioprobes derived from low-molecular-weight polypeptides or compounds, small recombinant antibody fragments (Fab, scFv), engineered variants (diabodies, triabodies, minibodies, and single-domain antibodies), or pretargeting antibody methods show rapid clearance of radioactivity from the circulation (*19–21*). Image-subtraction techniques (*22–24*) or kinetic model analysis (*25,26*) may also help solve this issue. Accordingly, ^{99m}Tc-TF-mAb or its derivatives have great potential as in vivo molecular imaging probes and deserve further investigation.

A higher renal accumulation of ^{99m}Tc-IgG$_1$ than of ^{99m}Tc-TF-mAb was observed in WHHLMI rabbits. Although an exact mechanistic explanation for this significant difference is not clear, several other investigators have also reported a relatively high renal accumulation after the injection of radiolabeled mAbs (*27–29*). Because we evaluated the biodistribution 24 h after the injection (relatively late phase), renal accumulation may be ascribed to metabolic or degradation products of ^{99m}Tc-labeled antibodies (*30*). Thus, further ex vivo metabolite analysis studies could help to clarify the mechanism. In addition, it is known that the excretion system of WHHLMI rabbits is compromised (*31*), which could alter the renal accumulation of tracers. On the other hand, although a certain degree of TF expression was observed in glomeruli (*32*), this could not be a reason for the higher renal accumulation of ^{99m}Tc-IgG$_1$.

Recently, the focus of anticoagulant research has turned to inhibition of the TF-FVIIa complex, and many pharmaceutical industry research programs have attempted to discover TF-FVIIa complex inhibitors (*33*). Studies in monkeys have indicated that inhibition of the TF-FVIIa complex, compared with other anticoagulants that inhibit thrombin or FXa, results in an improved profile . It is well known that the pathways for blood coagulation are interdependent, and the initiation, amplification, and propagation stages are closely regulated by positive and negative feedback loops. Thus, repeated doses of anticoagulants might increase the expression of ineffective (silent) TF complex in plaques because of such feedback processes independent of the antiatherosclerotic effect, although a lowering of net TF expression would be expected. The TF antibody we established in this study recognizes 193Ser-207Cys in the extracellular domain, which is distant from the protein sites related to complex formation with FVIIa. Therefore, the ^{99m}Tc-TF-mAb we developed can estimate the net TF expression in plaques, providing a useful tool to investigate the effect of such anticoagulants in vivo.

Comparison with Other Imaging Probes

In the search for suitable molecular probes to assess atherosclerotic lesion characteristics, many targets, including macrophage activity, angiogenesis, apoptosis, and cell tracking (monocyte, stem cell, lymphocyte), have been assessed (*1,2,34–36*). However, the usefulness of these probes is still under preliminary investigation, except for ^{18}F-FDG, a marker of inflammation, and ^{99m}Tc-annexin A5, a marker of ongoing apoptotic cell death, which are currently in clinical studies. In previous studies, we evaluated macrophage imaging using ^{18}F-FDG (*11*) and also ^{99m}Tc-LOX-1-mAb (*17*), which targets a scavenger receptor highly expressed on macrophages and foam cells and showed the usefulness for detection of atherosclerotic lesions. However, ^{18}F-FDG accumulated in relatively stable lesions because of the presence of macrophages in such lesions, as also seen in this report (Fig. 4). We also previously showed a certain degree of LOX-1 expression in relatively stable lesions with ^{99m}Tc-LOX-1-mAb. As for ^{99m}Tc-annexin A5, the accumulation ratios of atheromatous lesions to other lesions of ^{99m}Tc-TF-mAb (atheromatous to neointimal, 3.0; atheromatous to fibroatheromatous, 2.4; and atheromatous to collagen-rich, 2.9) were markedly higher than those of ^{99m}Tc-annexin A5 (atheromatous to neointimal,1.3; atheromatous to fibroatheromatous, 1.3; atheromatous to collagen-rich, 1.8) (*15*). Our previous study in apolipoprotein E–null mice also showed relatively high ^{18}F-FDG accumulation levels in early lesions, resulting in lower accumulation ratios for advanced to early lesions in comparison with ^{99m}Tc-annexin A5 (*37*). Thus, the desirable features of ^{99m}Tc-TF-mAb further confirm its potential as a molecular probe for detecting atheromatous lesions at higher risk for rupture.

CONCLUSION

In this study, we succeeded in determining TF expression using ^{99m}Tc-TF-mAb in WHHLMI rabbits. Consequently, we demonstrated prominently higher accumulation of ^{99m}Tc-TF-mAb in grade IV atheroma. These findings strongly indicate that molecular imaging of TF should provide clinically useful information on the thrombogenicity of atherosclerotic plaques.

ACKNOWLEDGMENTS

This work was partly supported by a grant-in-aid for general scientific research from the Ministry of Education, Culture, Sports, Science and Technology of Japan and from the Japan Society for the Promotion of Science and by a research grant from the Association for Nuclear Technology in Medicine and Takeda Science Foundation.

REFERENCES

1. Shaw SY. Molecular imaging in cardiovascular disease: targets and opportunities. *Nat Rev Cardiol.* 2009;6:569–579.
2. Saraste A, Nekolla SG, Schwaiger M. Cardiovascular molecular imaging: an overview. *Cardiovasc Res.* 2009;83:643–652.

3. Moons AH, Levi M, Peters RJ. Tissue factor and coronary artery disease. *Cardiovasc Res.* 2002;53:313–325.
4. Jeanpierre E, Le Tourneau T, Six I, et al. Dietary lipid lowering modifies plaque phenotype in rabbit atheroma after angioplasty: a potential role of tissue factor. *Circulation.* 2003;108:1740–1745.
5. Kuge Y, Kume N, Ishino S, et al. Prominent lectin-like oxidized low density lipoprotein (LDL) receptor-1 (LOX-1) expression in atherosclerotic lesions is associated with tissue factor expression and apoptosis in hypercholesterolemic rabbits. *Biol Pharm Bull.* 2008;31:1475–1482.
6. Shiomi M, Ito T, Yamada S, Kawashima S, Fan J. Development of an animal model for spontaneous myocardial infarction (WHHLMI rabbit). *Arterioscler Thromb Vasc Biol.* 2003;23:1239–1244.
7. Abrams MJ, Juweid M, tenKate CI, et al. Technetium-99m-human polyclonal IgG radiolabeled via the hydrazino nicotinamide derivative for imaging focal sites of infection in rats. *J Nucl Med.* 1990;31:2022–2028.
8. Ono M, Arano Y, Mukai T, et al. Plasma protein binding of ^{99m}Tc-labeled hydrazino nicotinamide derivatized polypeptides and peptides. *Nucl Med Biol.* 2001;28:155–164.
9. Larsen SK, Solomon HF, Caldwell G, Abrams MJ. [^{99m}Tc]tricine: a useful precursor complex for the radiolabeling of hydrazinonicotinate protein conjugates. *Bioconjug Chem.* 1995;6:635–638.
10. Ishii K, Kita T, Kume N, Nagano Y, Kawai C. Uptake of acetylated LDL by peritoneal macrophages obtained from normal and Watanabe heritable hyperlipidemic rabbits, an animal model for familial hypercholesterolemia. *Biochim Biophys Acta.* 1988;962:387–389.
11. Ogawa M, Ishino S, Mukai T, et al. ^{18}F-FDG accumulation in atherosclerotic plaques: immunohistochemical and PET imaging study. *J Nucl Med.* 2004;45:1245–1250.
12. Stary HC, Chandler AB, Glagov S, et al. A definition of initial, fatty streak, and intermediate lesions of atherosclerosis: a report from the Committee on Vascular Lesions of the Council on Arteriosclerosis, American Heart Association. *Circulation.* 1994;89:2462–2478.
13. Stary HC, Chandler AB, Dinsmore RE, et al. A definition of advanced types of atherosclerotic lesions and a histological classification of atherosclerosis: a report from the Committee on Vascular Lesions of the Council on Arteriosclerosis, American Heart Association. *Circulation.* 1995;92:1355–1374.
14. Kobayashi S, Inoue N, Ohashi Y, et al. Interaction of oxidative stress and inflammatory response in coronary plaque instability: important role of C-reactive protein. *Arterioscler Thromb Vasc Biol.* 2003;23:1398–1404.
15. Ishino S, Kuge Y, Takai N, et al. ^{99m}Tc-Annexin A5 for noninvasive characterization of atherosclerotic lesions: imaging and histological studies in myocardial infarction-prone Watanabe heritable hyperlipidemic rabbits. *Eur J Nucl Med Mol Imaging.* 2007;34:889–899.
16. Shiomi M, Ito T, Hirouchi Y, Enomoto M. Stability of atheromatous plaque affected by lesional composition: study of WHHL rabbits treated with statins. *Ann N Y Acad Sci.* 2001;947:419–423.
17. Ishino S, Mukai T, Kuge Y, et al. Targeting of lectinlike oxidized low-density lipoprotein receptor 1 (LOX-1) with ^{99m}Tc-labeled anti-LOX-1 antibody: potential agent for imaging of vulnerable plaque. *J Nucl Med.* 2008;49:1677–1685.
18. Shiomi M, Ito T, Hirouchi Y, Enomoto M. Fibromuscular cap composition is important for the stability of established atherosclerotic plaques in mature WHHL rabbits treated with statins. *Atherosclerosis.* 2001;157:75–84.
19. Huhalov A, Chester KA. Engineered single chain antibody fragments for radioimmunotherapy. *Q J Nucl Med Mol Imaging.* 2004;48:279–288.
20. Sharkey RM, Karacay H, Cardillo TM, et al. Improving the delivery of radionuclides for imaging and therapy of cancer using pretargeting methods. *Clin Cancer Res.* 2005;11:7109s–7121s.
21. Sano K, Temma T, Kuge Y, et al. Radioimmunodetection of membrane type-1 matrix metalloproteinase relevant to tumor malignancy with a pre-targeting method. *Biol Pharm Bull.* 2010;33:1589–1595.
22. Temma T, Iida H, Hayashi T, et al. Quantification of regional myocardial oxygen metabolism in normal pigs using positron emission tomography with injectable ^{15}O-O_2. *Eur J Nucl Med Mol Imaging.* 2010:37:377–385.
23. Yamamoto Y, de Silva R, Rhodes CG, et al. Noninvasive quantification of regional myocardial metabolic rate of oxygen by $^{15}O_2$ inhalation and positron emission tomography: experimental validation. *Circulation.* 1996;94:808–816.
24. Iida H, Rhodes CG, Araujo LI, et al. Noninvasive quantification of regional myocardial metabolic rate for oxygen by use of $^{15}O_2$ inhalation and positron emission tomography: theory, error analysis, and application in humans. *Circulation.* 1996;94:792–807.
25. Watabe H, Ikoma Y, Kimura Y, Naganawa M, Shidahara M. PET kinetic analysis: compartmental model. *Ann Nucl Med.* 2006;20:583–588.
26. Ikoma Y, Watabe H, Shidahara M, Naganawa M, Kimura Y. PET kinetic analysis: error consideration of quantitative analysis in dynamic studies. *Ann Nucl Med.* 2008;22:1–11.
27. Rogers BE, Anderson CJ, Connett JM, et al. Comparison of four bifunctional chelates for radiolabeling monoclonal antibodies with copper radioisotopes: biodistribution and metabolism. *Bioconjug Chem.* 1996;7:511–522.
28. Sugimoto K, Nishimoto N, Kishimoto T, Yoshizaki K, Nishimura T. Imaging of lesions in a murine rheumatoid arthritis model with a humanized anti-interleukin-6 receptor antibody. *Ann Nucl Med.* 2005;19:261–266.
29. D'Alessandria C, Malviya G, Viscido A, et al. Use of a ^{99m}Tc labeled anti-TNFα monoclonal antibody in Crohn's disease: in vitro and in vivo studies. *Q J Nucl Med Mol Imaging.* 2007;51:334–342.
30. Akizawa H, Arano Y. Altering pharmacokinetics of radiolabeled antibodies by the interposition of metabolizable linkages: metabolizable linkers and pharmacokinetics of monoclonal antibodies. *Q J Nucl Med.* 2002;46:206–223.
31. Campean V, Neureiter D, Varga I, et al. Atherosclerosis and vascular calcification in chronic renal failure. *Kidney Blood Press Res.* 2005;28:280–289.
32. Drake TA, Morrissey JH, Edgington TS. Selective cellular expression of tissue factor in human tissues: implications for disorders of hemostasis and thrombosis. *Am J Pathol.* 1989;134:1087–1097.
33. Prezelj A, Anderluh PS, Peternel L, Urleb U. Recent advances in serine protease inhibitors as anticoagulant agents. *Curr Pharm Des.* 2007;13:287–312.
34. Davies JR, Rudd JH, Weissberg PL, Narula J. Radionuclide imaging for the detection of inflammation in vulnerable plaques. *J Am Coll Cardiol.* 2006;47(8, suppl):C57–C68.
35. Jaffer FA, Libby P, Weissleder R. Molecular and cellular imaging of atherosclerosis: emerging applications. *J Am Coll Cardiol.* 2006;47:1328–1338.
36. Rudd JH, Hyafil F, Fayad ZA. Inflammation imaging in atherosclerosis. *Arterioscler Thromb Vasc Biol.* 2009;29:1009–1016.
37. Zhao Y, Kuge Y, Zhao S, et al. Comparison of ^{99m}Tc-annexin A5 with ^{18}F-FDG for the detection of atherosclerosis in ApoE−/− mice. *Eur J Nucl Med Mol Imaging.* 2007;34:1747–1755.

Erratum

In the article "^{18}F-FDG PET After 2 Cycles of ABVD Predicts Event-Free Survival in Early and Advanced Hodgkin Lymphoma," by Cerci et al. (*J Nucl Med.* 2010;51:1337–1343), Figure 4 contained a mistake. The graph of event-free survival in patients with a low International Prognostic Score should indicate that 10 of 18 patients (not 3 of 30) were PET2-positive. The authors regret the error.

特集　トランスレーショナルリサーチに貢献するウサギ

高コレステロール血症，心血管疾患に関するトランスレーショナルリサーチにおけるWHHLMIウサギの有用性

塩見　雅志，伊藤　隆
神戸大学 大学院 医学研究科 附属動物実験施設

1．はじめに

WHOの調査によると，WHO加盟国の死因の第一位は心血管疾患であり，死因の約30%を占めている。わが国では，死因の第一位は悪性新生物（がん），第2位が心血管疾患であり，心血管疾患はわが国においても克服しなければならない重要な疾患である。心血管疾患の危険因子として，高コレステロール血症，高血圧，糖代謝異常，喫煙，加齢，男性などが指摘されている。なかでも，血清脂質値の管理が重要とされており，現在の日本人の正常値は，血清総コレステロールの上限が220mg/dl，動脈硬化の原因になると考えられているLDL（低比重リポ蛋白）コレステロールの上限が140mg/dl，動脈硬化抑制因子であるHDL（高比重リポ蛋白）コレステロールの下限が40mg/dlとされている。1980年代以降の研究により，血清総コレステロール値と心血管疾患の発生率の間に高い相関があり，薬剤等で血清総コレステロール値を低下させると心血管疾患の発生を抑制できることが示された。コレステロール低下剤の開発は，日本の製薬会社（旧三共株式会社）が世界に先駆けて開発したコレステロール合成阻害剤（HMG-CoA還元酵素阻害剤，通称スタチン）が契機となり，その薬効評価に使用された実験動物が，故渡辺嘉雄先生（神戸大学）が開発されたWHHL（Watanabe heritable hyperlipidemic）ウサギであった[1]。旧三共株式会社の研究スタッフは，当初ラットを用いて薬効評価を実施したが，コレステロール低下作用は認められず開発を断念しかけていた。しかし，培養系とニワトリでの強いコレステロール合成阻害作用から，このスタチンの薬効を評価できる哺乳動物の探索を行なっていた。彼らによって麻布大学の紀要に掲載されていたWHHLウサギが見出され，WHHLウサギがスタチンの開発に貢献することになった。それは1979年のことであった。現在市場に出ているスタチンは7種類以上あり，世界中で2,000万人以上に処方される薬剤に成長し，スタチンの服用で心血管疾患による死亡率が対象群に比較して20～50%低下すると報告され，高脂血症や心血管疾患の治療に欠かせない薬剤となった。この経緯は，薬剤の開発というトランスレーショナルリサーチを遂行するに当たり，適切な動物種を選定することがいかに重要であるかを如実に物語っている。本総説では，WHHLMIウサギの開発過程とスタチンの開発におけるWHHLウサギのかかわりをとおして，トランスレーショナルリサーチにおける動物種選定の重要性を考えてみたい。

2．WHHLウサギ開発の歴史と特性

WHHLウサギは1973年に偶然発見された高脂血症を示す1匹のオスの日本白色種ウサギに由来する。8年間の交配実験を通して系統として確立された。当初，HLR（Hyperlipidemic rabbit）と命名され，その後開発者の名前を付すべきとの助言により，WHL（Watanabe-hyperlipidemic）ウサギと改名された。その後，動脈硬化の国際誌に投稿した際に編集者の一人からの助言で，WHHLウサギと命名された[2]。

系統として確立した当時のWHHLウサギは，成熟齢における血清総コレステロール値が300～700mg/dl，中性脂肪値が300～400mg/dlであり，大動脈に動脈硬化が発生し，四肢の指関節に黄色腫が発生した[1]。血圧，血糖値等は正常レベルであった。スタチンの開発に当たり，旧三共株式会社の研究スタッフはWHHLウサギの高脂血症の発症機序の解明を試みた。その結果，細胞表面に発現するLDL受容体の活性が顕著に低下し，血中からのLDLの異化が遅延し，血中にLDLが蓄積していることが明らかにされた[2,3]。これらの所見は，ヒトの家族性高コレステロール血症（FH）にきわめて類似しており，世界初のFHの自然発症のモデル動物であることが確認された。その後，1985年にノーベル賞を受賞したGoldstein JLとBrown MSの研究グループが，彼らが提唱していたリポ蛋白代謝におけるLDL受容体仮説をWHHLウサギを用いて証明した。彼らの研究によってヒトのリポ蛋白代謝が解明され，WHHLウサギのリポ蛋白代謝はヒトのリポ蛋白代謝に類似していることが明らかとなった。WHHLウサギ血中のリポ蛋白の組成および代謝がヒトに類似していたことから，WHHLウサギはコレステロール低下剤の開発研究に広く使用されるようになった。

高脂血症のモデル動物として重要なことは，ヒトの高脂血症で最後のイベントとなる心筋梗塞が発症することである。心筋梗塞の発症には心臓の冠動脈に動脈硬化が発生することが必須条件であるが，系統として確立した当時のWHHLウサギでは冠動脈の動脈硬化発生率はきわめて低値であった。神戸大学では冠動脈に動脈硬化が発生するWHHLウサギを開発するべく，選抜交配を実施し，1985年に冠動脈疾患を好発するWHHLウサギを開発し，1992年には重度の冠動脈病変が発生するWHHLウサギを開発した。しかし，心筋梗塞の発生率は改善されず低率であった。その後7年間の選抜交配の結果，動脈硬化による冠動脈の閉塞によって心筋梗塞が発生するWHHLMIウサギの開発に成功した[4]。これらの系統開発の過程で，大動脈と冠動脈の動脈硬化病変には質的に違いがあることが示唆され，冠動脈病変に対する薬剤の抑制効果を確認できる数少ない実験動物となった。しかし，WHHLウサギは開発過程によって冠動脈病変の発生状況が異なるため，どのステージのWHHLウサギであるかを確認する必要がある。なお，冠動脈に動脈硬化が安定して発生するWHHLウサギはWHHLMIウサギである。

これらの系統開発過程において，動脈硬化の発生機序の解明にWHHLウサギが用いられ，動脈硬化病変に酸化LDLが蓄積していること，LDLの酸化を抑制すると動脈硬化の発生・進展を抑制できること，動脈硬化が発生する際には動脈内皮にリンパ球接着因子が発現し，単球が接着して内皮下に侵入し，マクロファージとなって酸化LDLを貪食し，動脈硬化病変が形成されること等が解明された[2,3]。

3．脂質代謝，動脈硬化における種差

ウサギのリポ蛋白代謝はヒトに類似していることを上述した。リポ蛋白代謝がヒトと大きく異なれば，その動物種は脂質低下剤を開発する上で大きな障害となる。実験動物の代表であるマウスや

表1　ヒトの脂質代謝，動脈硬化，心機能解析等に対する高脂血症の遺伝子組換えマウスとウサギの類似性

	遺伝子組換 マウス*	WHHLMI ウサギ
脂質代謝		
血中の主要リポ蛋白	×（カイロミクロン，VLDL）	○（LDL）
内因性リポ蛋白の構造蛋白	×（apoB48）	○（apoB100）
アポB編集酵素の発現	×（小腸，肝）	○（小腸）
血中CETP活性	×（無）	○（有）
肝性リパーゼ	×（遊離）	○（血管壁に結合）
動脈硬化		
冠動脈	×（抵抗性）	△（自然発症）
病変の構成	×（脂質過剰蓄積）	○（種々の病変）
心臓		
心電図　四肢誘導	×（大きく異なる）	○（ヒトに類似）
胸部誘導	×（モニター困難）	○（ヒトに類似）
その他		
炎症マーカー	×（SAP）	○（CRP）
脂質低下剤**の効果	×（抵抗性）	○（有）

*apoE（−/−）マウス，LDLR（−/−）マウス
**スタチン（HMG-CoA還元酵素阻害剤，コレステロール合成阻害剤）

ラットでは脂質代謝がヒトと大きく異なる（表1）。マウス・ラットのリポ蛋白代謝でヒトやウサギと大きく異なる点は複数ある[2,3]。主な点は次のとおりである。1）apoB編集酵素が肝臓で発現する。その結果，ヒトやウサギの内因性リポ蛋白は構造蛋白としてapoB-100を有するが，マウスやラットでは外因性リポ蛋白と同じapoB-48を有する。apoB-48を持つリポ蛋白の代謝回転はきわめて速く，マウスやラットでは血中におけるリポ蛋白の構成がヒトと大きく異なる一因となっている。2）肝性リパーゼが血中に遊離している。その結果，中性脂肪の分解と遊離脂肪酸の組織への受け渡しがヒトと異なる。3）コレステロールエステル転送蛋白が発現していない。その結果，末梢組織から回収されたコレステロールがLDL等に渡されず，血中のHDLコレステロールの比率が増大し，血中のリポ蛋白の構成がヒトと大きく異なる。4）コレステロール合成の律速酵素の活性が強い。その結果コレステロール合成阻害剤に対して抵抗性を示す。したがって，マウスやラットの高脂血症のモデルでは血中に鬱滞しているリポ蛋白の種類がヒトと異なり，脂質低下剤の開発の障害になっている。また，ヒトの炎症マーカーであるC-反応性蛋白（CRP）はマウスやラットでは機能しておらず，動脈内皮細胞の機能にも差異が認められ，心筋線維の種類もヒトやウサギと異なることが知られている。さらに心電図所見もマウスやラットはヒトと大きく異なるがウサギはヒトに類似している。このようにマウスやラットでは脂質代謝や心血管疾患に関連する因子がヒトやウサギと大きく異なっている。したがって，マウスやラットをこれらの分野の実験に使用する場合には十分な配慮が必要となるであろう。

4．脂質低下剤の開発におけるトランスレーショナルリサーチ

WHHLウサギはリポ蛋白代謝がヒトにきわめて類似していることから，さまざまな脂質低下剤の開発に用いられてきた（表2）[2,3]。コレステロール合成阻害剤（コレステロール合成の上流に位置す

表2 WHHL／WHHLMIウサギを用いた薬剤開発研究

	脂質低下効果	動脈硬化抑制効果 大動脈	冠動脈
コレステロール合成阻害剤			
スタチン	○	×, ○	○
スクアレン合成阻害剤	○	○	○
陰イオン交換樹脂剤	○	○	
スタチン＋インイオン交換樹脂剤	○	○	○
MTP阻害剤	○		
ACAT阻害剤	×, ○	×, ○	×, ○
抗酸化剤			
プロブコール	○	○	
ビタミンE	×	×, ○	
コロニー刺激因子			
MCSF	×, ○	○	
GMCSF	×, ○	○	
アポE	×, ○	○	
フィブラート	×		
魚油，ω3脂肪酸	×, ○	×, ○	
チアゾリディンディオン	×	△	△
チアゾリディンディオン+スタチン	○	○	○
ACE阻害剤	×	○	
A-II受容体拮抗剤	×	○	
カルシウム拮抗剤	×	×	
βブロッカー	×	×	
遺伝子治療	○		

るHMG-CoA還元酵素や下流に位置するスクアレン合成酵素などの阻害剤），魚油等で代表されるω－3系脂肪酸，胆汁酸を吸着して腸－肝循環を遮断する陰イオン交換樹脂製剤，中性脂肪の低下作用を持つフィブラート系薬剤などの薬効が調べられ，コレステロール合成阻害剤と陰イオン交換樹脂製剤でコレステロール低下効果が確認されている。コレステロール合成阻害剤の一つであるスタチンを用いた研究では，投与用量に依存して血清総コレステロールが低下（対照群に比較して10～30％低下）した。コレステロール低下のメカニズムは，肝臓でのコレステロール合成抑制に伴うLDL受容体の増加による血中LDLの低下と，高用量の場合の肝からのVLDL（超低比重リポ蛋白）コレステロールの分泌低下の二つのメカニズムが関与していることが示唆された。スクアレン合成阻害剤も同様の作用機序で血清コレステロール値を低下させると考えられる。WHHLウサギはLDL受容体異常のdefective typeであることから，肝細胞におけるコレステロール合成阻害によって細胞表面に到達するLDL受容体蛋白が増加することが推測できる。陰イオン交換樹脂製剤は十二指腸で胆汁酸を吸着し腸－肝循環を遮断する。その結果，肝においてコレステロールが胆汁酸の材料として消費され，肝細胞がコレステロール不足となってLDL受容体が増加することが示されている。したがって，コレステロール合成阻害剤と陰イオン交換樹脂製剤の併用投与によって血清総コレステロール値は相加的に減少することもWHHLウサギを用いた研究で示されている。このことは，一般的

な高コレステロール血症に加えて，LDL受容体に異常があるヒトの家族性高コレステロール血症（除くLDL受容体ネガティブタイプ）においても，薬物治療が可能であることを示唆している。

5．脂質低下剤の動脈硬化抑制作用に関するトランスレーショナルリサーチ

血清総コレステロール値を低下させる目的は，動脈硬化を抑制し，心血管イベントや脳血管イベントを抑制することにある。コレステロール低下剤の投与によって動脈硬化が抑制できることがWHHLウサギを用いた研究で初めて証明された（表2）。スタチンを高用量で8ヵ月投与すると，血清総コレステロール値が20～30％低下し，冠動脈の狭窄率が対照群に比較して有意に低下した[5]。しかし，臨床における冠動脈造影による評価で，スタチンの投与で冠動脈狭窄率の改善が認められないケースにおいても心血管イベントの発生が有意に抑制できることが確認された。そのメカニズムの解明にもWHHLウサギが用いられた[6]。冠動脈にすでに動脈硬化が完成している成熟齢（10月齢）のWHHLウサギ（冠動脈病変好発系）にスタチンを1年間投与すると，冠動脈病変の進展抑制と同時に，動脈硬化病変中のマクロファージや脂質の蓄積の減少，コラーゲンなどの線維成分の増加と平滑筋細胞の減少の抑制が生じ，その結果，動脈硬化病変が破綻（病変が破れて血栓を生じる）しにくい安定な病変に質的に改善されることが明らかとなった。この研究によって，スタチンの動脈硬化病変安定化作用が心イベントの発生抑制に重要であることが確認された。スタチンの動脈硬化安定化作用が示されたことも一因となってスタチンの開発と処方される患者数は急激に増加した。また，動脈硬化の安定化が心イベントの抑制における重要な要素であることをvivoの実験で裏付けることができたことは，重要であった。コレステロール合成の下流部分を阻害するスクアレン合成阻害剤も同様の効果を示した。また，脂肪酸の質を換えて中性脂肪を低下させるω－3系脂肪酸，抗酸化剤，マクロファージの機能を調節する薬剤，アンギオテンシン系を阻害する薬剤などの動脈硬化抑制作用もWHHLウサギを用いて確認された[2,3]。このようにWHHLウサギは動脈硬化抑制作用に関する研究にきわめて有効である。

6．動脈硬化のイメージング

動脈硬化の進展を抑制あるいは治療する薬剤が開発された場合に必要になるのがヒトにおける薬効評価である。冠動脈病変の程度については冠動脈造影で病変の影を見ることができるが，び漫性に病変が広く発生している場合や冠動脈が動脈硬化によるリモデリングで外側に拡大している[7]場合には，病変の程度を判定することが困難となる。さらに，動脈硬化の破綻につながる危険な病変を非観血的に調べる技術と装置の開発は，治療効果の判定のみならず心血管イベントの発生予防においてもきわめて重要である。また，心血管イベントの原因になる動脈硬化病変として，マクロファージや脂質が蓄積したソフトプラークが重要と考えられており，このソフトプラークを検出する方法として，CT（Computed Tomography，コンピュータ断層撮影），PET（Positron Emission Tomography，陽電子放射断層撮影），CT＋PET，MR（Magnetic Resonance，核磁気共鳴），IVUS（Intravascular Ultrasound，血管内超音波エコー）などを用いた方法がWHHLMIウサギを用いて研究されている[2,3]。一例として，抗酸化剤をWHHLMIウサギに投与し，その動脈硬化抑制効果がCT＋PETで確認されている[8]。さらに研究が進み，動脈硬化病変のイメージング技術が確立すると，薬剤の効果の判定のみならず，心筋梗塞などの心血管イベントの原因になる危険性を持つ冠動脈病変

の検出が可能となり，虚血性心疾患の発生予防が可能になると期待できる。

7．今後の展望

脂質低下剤の開発や診断技術の開発研究が精力的に進められているが，心血管疾患の克服には未だ解決すべき様々な課題が残されている。とくに重要な課題として，冠動脈病変の破綻（動脈病変の破裂に伴う血栓の形成）による急性冠症候群の発生機序と予防法の解明，治療法の確立が待たれている。未だ，ヒトの急性冠症候群に対応したモデル動物は開発されていない。急性冠症候群のモデル動物の開発のために，WHHLMIウサギを用いて冠動脈病変の不安定化の亢進，冠動脈病変への物理的ストレス負荷などが試みられており[2, 3]，その実験結果が期待されている。冠動脈病変の不安定化においては，選抜交配による系統開発と共に遺伝子組換えWHHLMIウサギの開発が進められている[2, 3]。また，血清総コレステロール値が同程度であっても冠動脈病変の程度や発生する病変の質がウサギごとに異なることから，メタボロミクス解析によるマーカーや危険因子の解析も重要な課題となる。WHHLMIウサギを用いたメタボロミクス解析によって，心血管イベントに関係するマーカーや危険因子が明らかになれば，臨床における診断や発症予防に貢献できると期待できる。

8．まとめ

高コレステロール血症，動脈硬化，心血管イベントの治療，診断，予防に関するトランスレーショナルリサーチにWHHLウサギおよび心筋梗塞を発症するWHHLMIウサギは貢献してきた。心血管疾患による死亡が世界の死因の第一であることから，現在なお心血管疾患に関する研究は人類が克服すべき重要な疾患の一つであり，WHHLMIウサギは今後ともこの分野の研究に貢献するであろう。WHHLウサギは故渡辺嘉雄先生のご尽力と製薬会社のご支援で系統維持が行なわれ，世界各国の研究者に分与され，脂質代謝，動脈硬化，治療薬の開発等の研究に貢献してきた。神戸大学は現在なお年間100匹余のWHHLMIウサギの分与を継続している。バイオリソースとして30年余の歴史があるが，一研究機関の努力と民間支援のみで継続することには限界がある。日本で開発され，ノーベル賞研究に貢献し，心血管疾患のトランスレーショナルリサーチに活用されているWHHLMIウサギを次世代に引き継ぐためには，バイオリソース体制の確立が今後の課題である。

謝辞

本研究の一部は，厚生労働省科学研究費補助金創薬基盤推進研究事業（H20-生物資源-一般-002）により実施した。現在までにWHHLウサギあるいはWHHLMIウサギの系統維持を支援して戴いた旧三共株式会社，武田薬品工業株式会社，バイエル薬品株式会社，塩野義製薬株式会社，大正製薬株式会社，第一三共株式会社，大塚製薬株式会社，日本新薬株式会社，萬有製薬株式会社に深謝します。

参考文献

1) Watanabe Y. *Atherosclerosis* 1980; **36**: 261-268.
2) Shiomi M, Ito T. *Atherosclerosis* 2009; **207**: 1-7.
3) Shiomi M, Fun J. *Curr Opin Lipidol* 2008; **19**: 631-636.
4) Shiomi M, et al. *Arterioscler Thromb Vasc Biol* 2003; **23**: 1239-1244.
5) Watanabe Y, et al. *Biochim Biophys Acta* 1988; **960**: 294-302.
6) Shiomi M, et al. *Arterioscler Thromb Vasc Biol* 1995; **15**: 1938-1944.
7) Shiomi M, et al. *Atherosclerosis* 2008; **198**:287-293.
8) Ogawa M, et al. *J Nucl Med*. 2006; **47**:1845-1850.

特集　トランスレーショナルリサーチに貢献するウサギ

医学研究における遺伝子改変ウサギの応用とその展望

[1]範　江林，[1]小池　智也，[2]西島　和俊，[2]北嶋　修司
[1]山梨大学大学院医学工学総合研究部・分子病理学講座
[2]佐賀大学総合分析実験センター，生物資源開発部門

1．はじめに

Hammerらが1985年[1]に世界で初めてマイクロインジェクション法による遺伝子改変（Tg）ウサギの作製に成功して以来，25年を経た現在までに，Tgウサギの応用は先端的医学研究の，とくに心血管疾患や腫瘍，感染症などの研究分野において大きな役割を果たしてきた。しかし，汎用されているTgマウスと比し，Tgウサギの作製は世界で未だ，数箇所の研究施設に限られ，その応用もTgマウス程幅広く普及していないのが現状である。わが国においては，筆者らが1995年からスタートしたTgウサギの研究が各大学と実験動物業者らとの連携により，数多くの研究成果を発表すると共に，Tgウサギの作製，繁殖，系統維持，精子保存などのインフラ整備が世界に先駆けて確立されつつある[2]。さらに，2年毎に国内ウサギフォーラムや国際Tgウサギシンポジウムを主催しており，この研究分野においてすでに世界をリードしていると言える。本稿では，現在までに推進されているTgウサギの応用についてoverviewし，当面の問題点及び今後の展望についての持論を述べたい。

2．現在までのTgウサギの作製と応用の状況

図1に示すように1985年に初めてTgウサギが

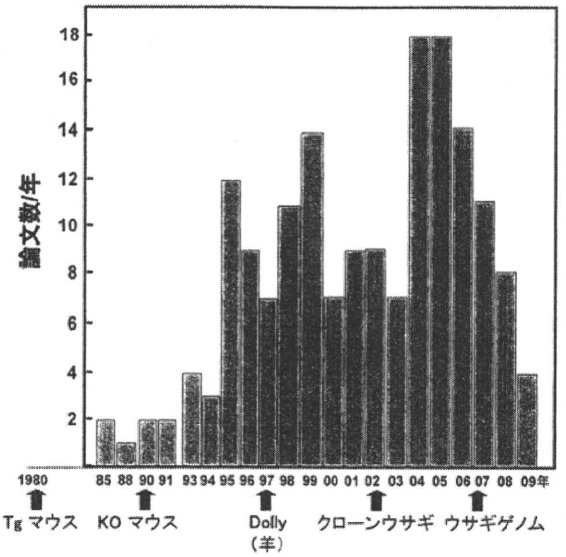

図1　これまでに発表されたTgウサギに関する英文論文（Pubmedより）

報告されてから，現在までにTgウサギに関する英文論文が約170編発表されている。90年代初頭，アメリカでは心臓血管病とりわけ動脈硬化及び脂質代謝研究のための新たな病態モデルとして，マウス以外の中型（ウサギ）並びに大型（ブタ）遺伝子改変動物の開発を推奨していた。当時は，筆者が所属していたカリフォルニア大学やベーラー医科大学，ペンシルベニア大学，シンシナティ大学及びNIH国立衛生研究所で同時にTgウサギの

表1 2010年3月までに100回以上引用されたTgウサギに関する論文（Google Scholarより）

論文名	引用回数
Hammer RE, et al. Production of transgenic rabbits, sheep and pigs by microinjection. *Nature*. 1985; **315**:680-683.	518
Patel R, et al. Simvastatin induces regression of cardiac hypertrophy and fibrosis and improves cardiac function in a transgenic rabbit model of human hypertrophic cardiomyopathy. *Circulation*. 2001; **104**:317-324.	258
Fan J, et al. Overexpression of hepatic lipase in transgenic rabbits leads to a marked reduction of plasma high density lipoproteins and intermediate density lipoproteins. *Proc Natl Acad Sci USA*. 1994; **91**:8724-8728.	181
Duverger N, et al. Inhibition of atherosclerosis development in cholesterol-fed human apolipoprotein A-I-transgenic rabbits. *Circulation*. 1996;**94**:713-717.	171
Hoeg JM, et al. Overexpression of lecithin:cholesterol acyltransferase in transgenic rabbits prevents diet-induced atherosclerosis. *Proc. Natl. Acad. Sci. USA*. 1996;**93**:11448-11453.	157
Yamanaka S, et al.Apolipoprotein B mRNA-editing protein induces hepatocellular carcinoma and dysplasia in transgenic animals. *Proc. Natl. Acad. Sci.USA*. 1995;**92**:8483-8487.	151
Shen J, et al. Macrophage-mediated 15-lipoxygenase expression protects against atherosclerosis development. *J Clin Invest*. 1996;**98**:2201-2208.	140
Nagueh SF, et al. Tissue Doppler imaging consistently detects myocardial contraction and relaxation abnormalities, irrespective of cardiac hypertrophy, in a transgenic rabbit model of human hypertrophic cardiomyopathy. *Circulation*. 2000;**102**:1346-1350.	131
Marian AJ, et al. A transgenic rabbit model for human hypertrophic cardiomyopathy. *J Clin Invest*. 1999; **104**:1683-1692.	128
Serhan CN, et al. Reduced inflammation and tissue damage in transgenic rabbits overexpressing 15-lipoxygenase and endogenous anti-inflammatory lipid mediators. *J Immunol*. 2003;**171**:6856-6865.	121
Van den Hout JM, et al. Enzyme therapy for pompe disease with recombinant human alpha-glucosidase from rabbit milk. *J Inherit Metab Dis*. 2001;**24**:266-274.	110

開発が行なわれた。それ故，90年代半ば頃，Tgウサギ論文の発表数が急増している。現在までに発表されたTgウサギの論文数は決して多いとはいえないが，100回以上引用された論文を検索すると，計11編あり（表1），ほとんどが一流雑誌に掲載されている。また，その研究内容を見ると，Tgウサギの使用目的は，脂質代謝や動脈硬化，心臓病の研究が大半であった。しかし，2003年のイラク戦争以降は，アメリカ政府からの研究経費が大幅に減額されたため，アメリカでのTgウサギ研究が縮小されつつあり，現在，Tgウサギが作製できる施設はペンシルベニア大学のみとなっている。幸いに，わが国とヨーロッパ諸国（ハンガリー，フランス，ドイツ，スロバキア）においてはこの研究を継続できる環境にあったため，現在では牽引的な役割を果たしている。とくに筆者らは主導的な立場として国内外のウサギフォーラムを企画し，実行してきた。国内においては2003年に初めて，佐賀大学で開催した第1回「医療に貢献する実験用ウサギの新しい展開」を皮切りに，第2回（2006年，山梨大学），第3回（2008年，神戸大学），第4回（2010年，秋田大学・予定）と継続して開催している。同時に，2005年に第1回遺伝子改変ウサギ国際シンポジウムを筑波大学で主催し，続いて，2007年第2回（Jouy en Josas, France），2009年第3回（西安，中国）と行ない，次回第4回（2011年ブダペスト，ハンガリー）も現在準備中である。また，2007年12月には，アメリカハーバード大学にあるBroad研究所で，初めてのウサギゲノム共同体会議も開催された。

上述のごとく，Tgウサギを開発する主な目的はヒトの病態モデルとしての応用である[3]。とくに高脂血症や動脈硬化，糖尿病，心筋症，不整脈などの研究におけるTgウサギの役割が極めて重要なポイントである。なぜマウスではなく，ウサギを使うかという大きな理由は，ウサギが，ヒトと類似している独特の生理機能を有していることと，遺伝子の導入によりヒトの病態を忠実に再現できることが挙げられる。例えば，ウサギの主要な血清リポ蛋白はLDLであり，リポ蛋白代謝に必要な転送蛋白CETPも有しているために，動脈硬化になりやすい特徴がある。ちなみに，マウスはヒトと違って，血清リポ蛋白がHDLであり，CETPも欠損している。また，心筋細胞の特徴においても，ウサギの心筋繊維のmyosin heavy chainはヒトと同様β型であり，心筋症や不整脈のモデルとして最適であることが報告されている。一方で心筋繊維がα型のマウスは心筋症や不整脈が発生できないとされている。しかし，疾患モデルによる動物実験の最終目的は，その研究成果をいかに人間の病気の治療及び診断法の開発へと発展させられるかがもっとも重要である。その意味で，どのようなモデルを使い，どういった研究成果を出し，その研究成果がトランスレーショナル（実用的な臨床への橋渡し研究，from bench to bedside研究）かどうかが最大の課題となり，その点において，Tgウサギの貢献が大いに期待されている。

Tgウサギを用いるもう一つの目的は，ウサギを“動物工場”として利用し，治療用の生物活性蛋

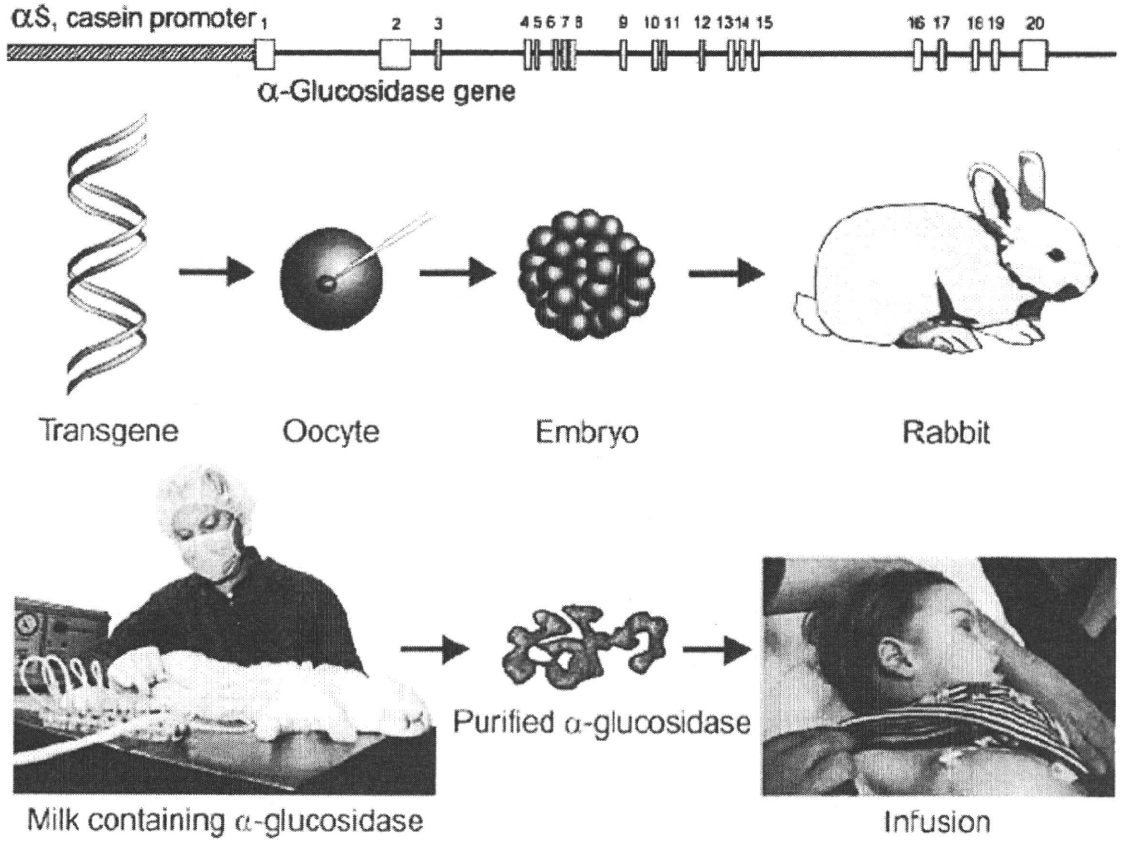

図2　Tgウサギより精製されたαグルコシダーゼを用いたヒト糖原蓄積症に対する治療法（参考文献4より）